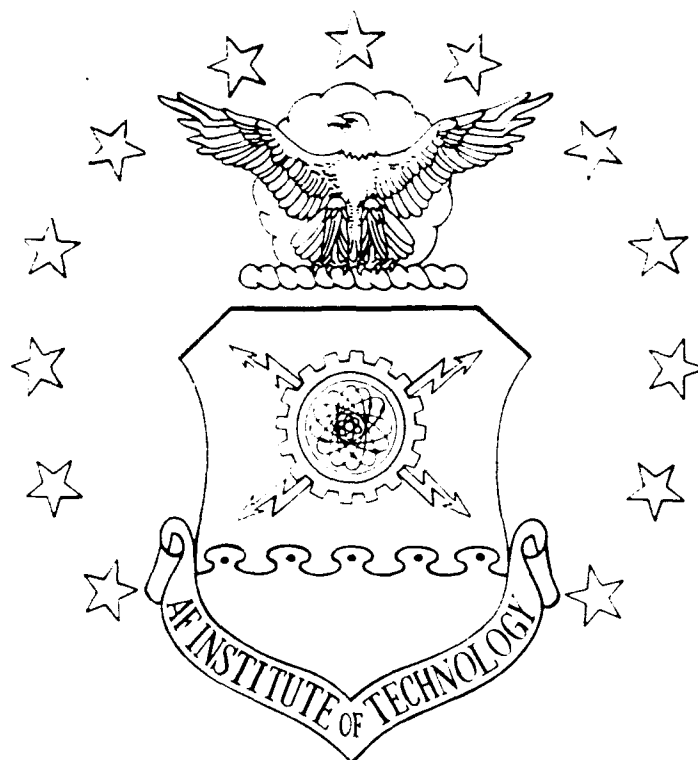


AD-A230 683



AUTONOMOUS NAVIGATION
OF A
SATELLITE CLUSTER

THESIS

Stephen C. Johnston, Captain, USAF

AFIT/GA/ENY/90D-9

DEPARTMENT OF THE AIR FORCE
AIR UNIVERSITY

AIR FORCE INSTITUTE OF TECHNOLOGY

DTIC
ELECTE
JAN 03 1991

D

Wright-Patterson Air Force Base, Ohio

DISTRIBUTION STATEMENT A

Approved for public release
Distribution Unlimited

AFIT/GA/ENY/90D-9

AUTONOMOUS NAVIGATION
OF A
SATELLITE CLUSTER

THESIS

Stephen C. Johnston, Captain, USAF

AFIT/GA/ENY/90D-9

Approved for public release; distribution unlimited

AFIT/GA/ENY/90D-9

AUTONOMOUS NAVIGATION
OF A
SATELLITE CLUSTER

THESIS

Accession For	
NTIS GRA&I	<input checked="checked" type="checkbox"/>
DTIC TAB	<input type="checkbox"/>
Unannounced	<input type="checkbox"/>
Justification	
By	
Distribution/	
Availability Codes	
Dist	Avail and/or Special
A-1	

Presented to the Faculty of the School of Engineering
of the Air Force Institute of Technology
Air University
In Partial Fulfillment of the
Requirements for the Degree of
Master of Science in Astronautical Engineering

Stephen C. Johnston, B.S.
Captain, USAF

December, 1990

Approved for public release; distribution unlimited



Preface

This study investigated the state observability problems associated with a previously developed on-board recursive filter that estimates the relative position of each satellite within a satellite cluster. A non-linear least squares filter was used to find and remove the unobservable components of the state. The on-board filter's performance was reinvestigated with the updated state equations.

My heartfelt appreciation and thanks go to Dr. William Wiesel and Dr. Rodney Bain for providing my greatest enjoyment at AFIT, their astrodynamics classes. Additional thanks go to Dr. Wiesel, my thesis advisor, for his support and guidance in completing this thesis. My deepest love and thanks go to my wife Christy who followed me to Dayton, Ohio and endured, once again, the life of a student. I give my greatest love and thanks to the greatest joy in my life, my sons Greg and Andrew. My special thanks and love go to my parents, Hugh and Shirley Johnston for their many years of love, guidance, and support.

Stephen C. Johnston

Table of Contents

	Page
Preface	ii
List of Figures	iv
Abstract	vi
I. Introduction	1
II. Background	4
2.1 Truth Model	4
2.2 Kalman Filter	11
2.2.1 Dynamics	14
2.2.2 U-D Covariance Factorization Filter	16
2.3 State Definition	19
III. Observability Analysis	23
3.1 Non-Linear Least Squares Estimation	23
3.2 Analysis	24
IV. Performance Analysis	32
4.1 Filter Tuning	33
4.2 Monte Carlo Simulation	37
4.2.1 Two Satellite Constellation	39
4.2.2 Five Satellite Constellation	41
4.2.3 Ten Satellite Constellation	48
V. Conclusions and Recommendations	55
Bibliography	57
Vita	59

List of Figures

Figure	Page
1. Reference System	5
2. True Error and Covariance as a Function of Time with zero dynamics noise	34
3. True Error and Covariance as a Function of Time with Dynamics Noise on the order of $2.25 \times 10^{-14} \text{KM}^2/\text{SEC}^2$	36
4. Filter Tuned with Dynamics Noise Covariance of $9 \times 10^{-18} \text{KM}^2/\text{SEC}^2$	37
5. Average Error for a Two Satellite Constellation	40
6. Comparison of Average True Error and Covariance Versus Time for a Two Satellite Constellation	41
7. Average Error Between Satellites 1 and 2	43
8. Comparison of Average True Error and Covariance Versus Time for Satellites 1 and 2	44
9. Average Error Between Satellites 1 and 3	45
10. Comparison of Average True Error and Covariance Versus Time for Satellites 1 and 3	46
11. Average Error Between Satellites 1 and 5	47
12. Comparison of Average True Error and Covariance Versus Time for Satellites 1 and 5	47

Figure	Page
13. Average Error Between Satellites 1 and 2	49
14. Comparison of Average True Error and Covariance Versus Time for Satellites 1 and 2	50
15. Average Error Between Satellites 1 and 5	51
16. Comparison of Average True Error and Covariance Versus Time for Satellites 1 and 5	52
17. Average Error Between Satellites 1 and 10	53
18. Comparison of Average True Error and Covariance Versus Time for Satellites 1 and 10	54

ABSTRACT

The relative position determination of a cluster of satellites operating in a low earth orbit is investigated. A U-D Covariance Factorization Kalman Filter is used for the on-board estimator with dynamics based on the Clohessy-Wiltshire equations. Measurements consist of range data between a single host satellite and the remaining cluster. Therefore only relative position and velocity states with respect to the host satellite can be determined. A 15-sample Monte Carlo simulation was conducted with clusters of 2, 5 and 10 satellites, respectively. Performance results consist of average error, average true error and filter covariance as a function of time.

AUTONOMOUS NAVIGATION
OF A
SATELLITE CLUSTER

I. Introduction

The concept of using a recursive filter for relative position determination for a cluster of satellites acting as a space based radar was the topic of two previous Air Force Institute of Technology masters' theses. The initial concept called for a cluster of up to ten satellites orbiting in a near circular, low earth orbit. The cluster was placed within a volume of space of dimensions 500 X 500 X 500 meters³ and the accuracy requirement of the filter was 25 meters. The accuracy was based upon the requirement to form a clear, cohesive image and is a function of the radar's wavelength. The filter operated on range data determined from synchronized clock pulses.

Captain Michael L. P. Ward investigated the feasibility of using a recursive filter to determine the relative position of each satellite within the cluster. The filter was a U-D covariance factorization Kalman filter. During testing, Captain Ward discovered that the downrange component of the state was unobservable (6:2-17). The

cluster's state was therefore modified to include only relative downrange components. The filter's performance satisfied the required accuracy and proved promising under initial testing (6:4-1). The continued testing of the filter was conducted by Captain Sherrie Norton Filer.

Captain Filer investigated the discrepancy between the results from each satellite (3:2). Captain Ward's initial testing revealed that filter performance was different for each satellite. The satellite that contains the filter under investigation is defined as the host satellite. During continued research, Captain Filer discovered that the filter for the host satellite, designated satellite #1, was unable to update its state vector components. Additional information was sent to satellite #1's filter in an effort to improve its ability to update its own state. When this effort proved unsuccessful, Captain Filer initiated a search for other unobservable state components. The research yielded mixed results; it seems that none of the states were truly unobservable (3:52).

The purpose of this thesis is to continue the investigation into the unobservability of the state components. The orbital altitude, cluster radius, and accuracy requirement will remain the same. The cluster geometry will be a random distribution of satellites within

the cluster volume. Satellite #1 will be considered the primary satellite and its filter's performance will be the source of the results presented in this thesis. Extensive usage of Captains Ward and Filer's computer code will be made in an effort to reduce development and testing time.

II. Background

The U-D covariance factorization filter computer code was originally generated by Captain Ward. Additionally, a truth model was developed to provide the estimator with perfect or corrupted range data and to provide a true state for comparison against the estimator's state. The following sections detail the development of the truth model and the estimator as previously presented by Captain Ward (6:2-1-2-21).

2.1 Truth Model

The truth model was based on two-body orbital dynamics and provided the cluster's true state and the relative distance between each satellite. The range data is a relative measurement and therefore absolute positions cannot be determined by the estimation filter. Alternatively, the relative distance is defined with respect to a rotating reference point located in a circular orbit of radius R with velocity $\sqrt{\mu/R}$. The rotating reference frame $(\hat{x}, \hat{y}, \hat{z})$ rotates with respect to an earth-centered inertial reference frame $(\hat{i}, \hat{j}, \hat{k})$ at a constant angular rate of $\omega \hat{k}$ (see Figure 1).

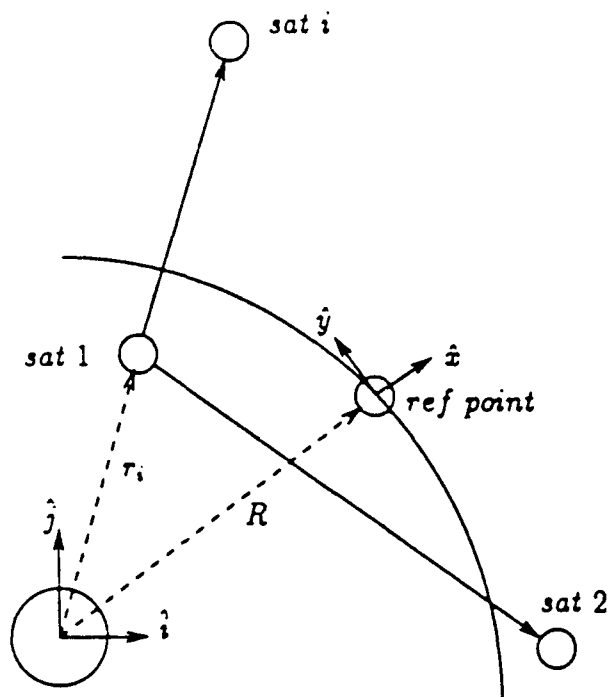


Figure 1. Reference System. (3:5).

The reference point's initial position and velocity are:

$$r_{ref} = \begin{Bmatrix} R \\ 0 \\ 0 \end{Bmatrix} \quad (1)$$

$$v_{ref} = \begin{pmatrix} 0 \\ \sqrt{\frac{\mu}{R}} \\ 0 \end{pmatrix} \quad (2)$$

The position of each satellite within the cluster was defined randomly about the reference point and takes the form:

$$r_i = \begin{pmatrix} R \\ 0 \\ 0 \end{pmatrix} + \{n_i\} * (500 \text{ meters}) \quad (3)$$

where n_i is a vector of random numbers between -0.5 and 0.5 from a uniformly distributed random number generator.

The radial and out-of-plane components of a satellite's velocity are determined by the Clohessy-Wiltshire equations (these equations will be introduced in the next section) and take the form: (8:80)

$$v_i \hat{l} = \eta (r_i \hat{l} - r_{ref} \hat{l}) \quad (4)$$

$$v_i \hat{k} = \eta r_i \hat{k} \quad (5)$$

where η is the mean motion of the reference point.

The third component of the satellite's velocity is determined from the constraint that the orbital periods of all satellites within the cluster must be equal to ensure that the cluster remains intact. From Kepler's laws, the orbital period of an elliptical orbit is a function of the semi-major axis of the orbit (2:33). Therefore, the semi-major axis of each satellite must be the same and equal to the radius of the reference point. Utilizing the energy equation, one may solve for the third velocity component to obtain:

$$v_i \hat{j} = \sqrt{2\mu \left(\frac{1}{r_i} - \frac{1}{2}a \right) - v_i \hat{i} \cdot v_i \hat{i} - v_i \hat{k} \cdot v_i \hat{k}} \quad \hat{j} \quad (6)$$

The above information may be used to form the inputs to the estimator. Captain Ward defined the initial true state as the position and velocity components of each satellite expressed with respect to the rotating reference frame [ROT]. Initially, the axes of both the fixed, inertial frame [FIX] and the rotating frame are aligned and the position and velocity may be expressed as:

$$\mathbf{r}_{i[\text{ROT}]} = (\mathbf{r}_i - \mathbf{r}_{ref})_{[\text{FIX}]} \quad (7)$$

$$\mathbf{v}_{i[\text{ROT}]} = (\mathbf{v}_i - \mathbf{v}_{ref})_{[\text{FIX}]} - \boldsymbol{\omega} \times \mathbf{r}_{i[\text{ROT}]} \quad (8)$$

therefore the state at $t=0$ is

$$\mathbf{X}_t(0) = \begin{bmatrix} \mathbf{r}_{1[\text{ROT}]} \\ \mathbf{v}_{1[\text{ROT}]} \\ \cdot \\ \cdot \\ \cdot \\ \mathbf{r}_{s[\text{ROT}]} \\ \mathbf{v}_{s[\text{ROT}]} \end{bmatrix} \quad (9)$$

Additionally, the truth model outputs an $s-1$ relative measurement vector.

$$\mathbf{z}_t = \begin{bmatrix} |r_1 - r_2| \\ \cdot \\ \cdot \\ \cdot \\ |r_1 - r_s| \end{bmatrix} + \mathbf{u}_t \quad (10)$$

where \mathbf{u}_t represents zero-mean, white Gaussian noise with an associated covariance of \mathbf{R}_t (4:330). The noise \mathbf{u}_t is the best representation for errors in computing the range measurements from the clock pulses. There are numerous sources for the errors, but for the purpose of this thesis

the errors are lumped together into a single term and considered independent from measurement to measurement (6:2-6).

The future position and velocity vectors for each satellite are determined by the solution of the Kepler problem and the f and g equations defined in terms of the eccentric anomaly E (2:219). The equations take the following form:

$$f = 1 - \frac{a}{r_o} (1 - \cos \Delta E) \quad (11)$$

$$g = t - \sqrt{\frac{a^3}{\mu}} (\Delta E - \sin \Delta E) \quad (12)$$

$$\dot{f} = \frac{\sqrt{\mu a} \sin \Delta E}{r r_o} \quad (13)$$

$$\dot{g} = 1 - \frac{a}{r} (1 - \cos \Delta E) \quad (14)$$

where ΔE and r are defined as:

$$\Delta E = E_f - E_o \quad (15)$$

$$r = a(1 - e \cos E_f) \quad (16)$$

The value of the eccentric anomaly, E_f , for any time t was determined by a Newton iteration scheme due to the

transcendental nature of the Kepler equation. Once f, g, \dot{f} , and \dot{g} are determined, the new position and velocity vectors for each satellite may be calculated using:

$$r(t) = fr_o + gv_o \quad (17)$$

$$v(t) = \dot{f}r_o + \dot{g}v_o \quad (18)$$

Once the position and velocity of each satellite with respect to the inertial reference frame have been determined, the relative position and velocity vectors with respect to the rotating reference frame can be determined. First, the new inertial position and velocity vectors of the reference point must be determined. This is easily accomplished by a rotation about the \hat{k} axis through an angle θ defined as:

$$\theta = \omega \cdot t \quad (19)$$

Therefore, the new inertial position and velocity vectors for the reference point are:

$$r_{ref[fix]}(t) = \begin{bmatrix} R \cos \theta \\ R \sin \theta \\ 0 \end{bmatrix} \quad (20)$$

$$v_{ref[fix]}(t) = \begin{bmatrix} -\sqrt{\frac{\mu}{R}} \sin \theta \\ \sqrt{\frac{\mu}{R}} \cos \theta \\ 0 \end{bmatrix} \quad (21)$$

The inertial, relative position and velocity vectors between each satellite and the reference point are determined by subtracting the two solutions.

$$r_{rel[fix]} = [r(t) - r_{ref}(t)] = r_1 \hat{i} + r_2 \hat{j} + r_3 \hat{k} \quad (22)$$

$$v_{rel[fix]} = [v(t) - v_{ref}(t)] = v_1 \hat{i} + v_2 \hat{j} + v_3 \hat{k} \quad (23)$$

Since the inertial and the rotating reference frames are no longer aligned, eqns (22) and (23) must undergo a coordinate transformation through the angle θ as previously defined. The relative position and velocity vectors expressed with respect to the rotating reference frame are:

$$\begin{bmatrix} r_{1[ROT]} \\ v_{1[ROT]} \end{bmatrix} = \begin{bmatrix} r_1 \cos \theta + r_2 \sin \theta \\ -r_1 \sin \theta + r_2 \cos \theta \\ r_3 \\ v_1 \cos \theta + v_2 \sin \theta + \omega \cdot r_2 \\ -v_1 \sin \theta + v_2 \cos \theta - \omega \cdot r_1 \\ v_3 \end{bmatrix} \equiv \begin{bmatrix} x \\ y \\ z \\ \dot{x} \\ \dot{y} \\ \dot{z} \end{bmatrix} \quad (24)$$

Once the position vectors expressed in the rotating reference frame have been determined, the filter inputs can be calculated as before.

2.2 Kalman Filter

The extended Kalman filter is used due to the nonlinear nature of the measurements. The 'U-D covariance factorization' version of the Kalman filter was used to

solve numerical problems encountered by Captain Ward (6:2-14). This form of the Kalman filter will continue to be used for the estimator once the observability problems are identified and corrected.

The system's state propagation is described in terms of a linear stochastic differential equation. The available filter inputs are discrete-time, noise corrupted, nonlinear measurements of the range between the satellites. The Kalman propagation equations for the system are (4:220):

$$\hat{x}(t_i^-) = \Phi(t_i, t_{i-1}) \hat{x}(t_{i-1}^+) \quad (25)$$

$$P(t_i^-) = \Phi(t_i, t_{i-1}) P(t_{i-1}^+) \Phi^T(t_i, t_{i-1}) + G_d(t_{i-1}) Q_d(t_{i-1}) G_d^T(t_{i-1}) \quad (26)$$

Where

Q_d = The covariance of the dynamics driving noise.

$\hat{x}(t_i^-)$ = The estimated state after time propagation.

$\hat{x}(t_i^+)$ = The estimated state after the measurement update.

G_d = Equals the identity matrix (because the model is an equivalent discrete-time representation of a continuous-time system (4:377))

Φ = The state transition matrix.

The time argument (t_i^+) will be replaced by (\pm) for the remainder of the text. The first time propagation occurs before any measurement updates, thus the initial filter state and covariance must be established (6:2-10). For

ease in studying the steady state behavior of the filter, \hat{x}_0 will be set equal to $x_i(0)$. The initial state covariance matrix P_0 will be diagonal with position elements of order $10^{-6} km^2$ and velocity elements of order $10^{-12} km^2/sec^2$ respectively.

The extended Kalman filter update equations are (5:44)

$$\hat{x}(+) = \hat{x}(-)K\{z - h[\hat{x}(-)]\} \quad (27)$$

$$P(+) = P(-) - KHP(-) \quad (28)$$

K is the Kalman filter gain; an expression defining the gain will be developed shortly.

The measurement vector $h(\hat{x}, t)$ is the filter's estimate of the range between the satellites. Therefore, the residual is the difference between the observed data vector and the measurement vector, $z - h[\hat{x}(-)]$. The measurement vector's form is:

$$h = \begin{bmatrix} \sqrt{(x_1 - x_2)^2 + (y_1 - y_2)^2 + (z_1 - z_2)^2} \\ \vdots \\ \sqrt{(x_1 - x_s)^2 + (y_1 - y_s)^2 + (z_1 - z_s)^2} \end{bmatrix} = \begin{bmatrix} h_1 \\ \vdots \\ h_{s-1} \end{bmatrix} \quad (29)$$

The matrix H is developed from linearizing the h vector with respect to the state components and evaluating it after the time propagation of the state, $\hat{x}(-)$:

$$H = \left. \frac{\partial h}{\partial \mathbf{x}} \right|_{\mathbf{x}=\hat{\mathbf{x}}(-)} \quad (30)$$

Which has the following form:

$$H = \begin{bmatrix} H_1 & -H_1 & 0 & \dots & 0 \\ H_2 & 0 & -H_2 & \dots & 0 \\ \cdot & \cdot & \cdot & \cdot & \cdot \\ \cdot & \cdot & \cdot & \cdot & \cdot \\ \cdot & \cdot & \cdot & \cdot & \cdot \\ H_{s-1} & 0 & 0 & \dots & -H_{s-1} \end{bmatrix} \quad (31)$$

where

$$H_1 = \begin{bmatrix} \frac{x_1 - x_2}{h_1} & \frac{y_1 - y_2}{h_1} & \frac{z_1 - z_2}{h_1} & 0 & 0 & 0 \end{bmatrix} \quad (32)$$

$$H_{s-1} = \begin{bmatrix} \frac{x_1 - x_s}{h_{s-1}} & \frac{y_1 - y_s}{h_{s-1}} & \frac{z_1 - z_s}{h_{s-1}} & 0 & 0 & 0 \end{bmatrix} \quad (33)$$

2.2.1 Dynamics

The system dynamics, i.e. the state transition matrix, is based upon the Clohessy-Wiltshire equations of motion. These equations describe "the relative motion of two satellites when one is in a circular orbit." (8:78):

$$\ddot{x} - 2\eta\dot{y} - 3\eta^2 x = 0 \quad (34)$$

$$\ddot{y} + 2\eta\dot{x} = 0 \quad (35)$$

$$\ddot{z} + \eta^2 z = 0 \quad (36)$$

One may integrate these equations about the initial conditions $x_o, \dot{x}_o, y_o, \dot{y}_o, z_o, \text{ and } \dot{z}_o$ to obtain the position and velocity solutions (8:79-81)

$$x(t) = -\left(\frac{2}{\eta}\dot{y}_o + 3x_o\right)\cos\eta t + \frac{\dot{x}_o}{\eta}\sin\eta t + 4x_o + \frac{2}{\eta}\dot{y}_o \quad (37)$$

$$y(t) = y_o - (3\dot{y}_o + 6\eta x_o)t + \left(\frac{4\dot{y}_o}{\eta} + 6x_o\right)\sin\eta t + \frac{2\dot{x}_o}{\eta}\cos\eta t - \frac{2\dot{x}_o}{\eta} \quad (38)$$

$$z(t) = z_o\cos\eta t + \frac{\dot{z}_o}{\eta}\sin\eta t \quad (39)$$

$$\dot{x}(t) = (2\dot{y}_o + 3\eta x_o)\sin\eta t + \dot{x}_o\cos\eta t \quad (40)$$

$$\dot{y}(t) = -3\dot{y}_o - 6\eta x_o + (6\eta x_o + 4\dot{y}_o)\cos\eta t - 2\dot{x}_o\sin\eta t \quad (41)$$

$$\dot{z}(t) = -z_o\eta\sin\eta t + \dot{z}_o\cos\eta t \quad (42)$$

Now, one may develop the state transition matrix (8:81).

$$\Phi = \begin{bmatrix} 4-3\cos\psi & 0 & 0 & \frac{\sin\psi}{\eta} & \frac{2}{\eta}(1-\cos\psi) & 0 \\ 6(\sin\psi-\psi) & 1 & 0 & \frac{2}{\eta}(\cos\psi-1) & \frac{4}{\eta}\sin\psi - \frac{3\psi}{\eta} & 0 \\ 0 & 0 & \cos\psi & 0 & 0 & \frac{\sin\psi}{\eta} \\ 3\eta\sin\psi & 0 & 0 & \cos\psi & 2\sin\psi & 0 \\ 6\eta(\cos\psi-1) & 0 & 0 & -2\sin\psi & -3+4\cos\psi & 0 \\ 0 & 0 & -\eta\sin\psi & 0 & 0 & \cos\psi \end{bmatrix} \quad (43)$$

where ψ is $\eta\delta t$ and δt is the sample time. Generalizing the state propagation equation for the s satellites yields

$$\hat{x}(+) = \begin{bmatrix} \phi_1 & 0 & 0 & \cdot & \cdot & 0 \\ 0 & \phi_2 & 0 & \cdot & \cdot & 0 \\ 0 & 0 & \phi_3 & \cdot & \cdot & 0 \\ \cdot & \cdot & \cdot & \cdot & \cdot & \cdot \\ \cdot & \cdot & \cdot & \cdot & \cdot & \cdot \\ 0 & 0 & 0 & \cdot & \cdot & \phi_s \end{bmatrix} \begin{pmatrix} \hat{x}_1 \\ \hat{x}_2 \\ \hat{x}_3 \\ \cdot \\ \cdot \\ \hat{x}_s \end{pmatrix} \quad (44)$$

2.2.2 U-D Covariance Factorization Filter

The U-D filter is especially valuable for small word length micro-processors, since it achieves twice the numerical precision capability for the same wordlength (4:400). The basis of the filter is the factorization of the covariance matrices into a unitary upper triangular and a diagonal matrix, such that

$$P(-) = U(-)D(-)U^T(-) \quad (45)$$

$$P(+) = U(+)D(+)U^T(+) \quad (46)$$

The algorithm is initiated with the same initial covariance values as stated above. First, the initial n -by- n covariance matrix P_0 (where n is the number of states) is factored into the UDU^T form by the following steps:

First, for the n^{th} column determine

$$D_{nn} = P_{nn} \quad (47)$$

$$U_{in} = \begin{cases} 1 & i = n \\ P_{in}/D_{nn} & i = n-1, n-2, \dots, 1 \end{cases} \quad (48)$$

Then for the remaining columns, $j = n-1, n-2, \dots, 1$ determine

$$D_{jj} = P_{jj} - \sum_{k=j+1}^n D_{kk} U_{jk}^2 \quad (49)$$

$$D_{ij} = \begin{cases} 0 & i > j \\ 1 & i = j \\ \left[P_{ij} - \sum_{k=j+1}^n D_{kk} U_{ik} U_{jk} \right] / D_{jj} & i = j-1, j-2, \dots, 1 \end{cases} \quad (50)$$

Once the initial U and D matrices are determined, the state can be propagated forward to the first update time. The n -by- $2n$ matrix $Y(-)$ is formed by augmenting the state propagation equation and the identity matrix G_d .

$$Y(-) = [\Phi U(+)|G_d] \quad (51)$$

Finally, the $2n$ -by- $2n$ matrix $\tilde{D}(-)$ is formed by using the $D(+)$ and Q_d matrices as the block diagonal elements.

$$\tilde{D}(-) = \begin{bmatrix} D(+) & 0 \\ 0 & Q_d \end{bmatrix} \quad (52)$$

The transpose of the $Y(-)$ matrix forms a matrix of column vectors a_i of length $2n$.

$$Y^T(-) = [a_1 \quad a_2 \quad \dots \quad a_n] \quad (53)$$

The propagation is accomplished by calculating the following relationships for $k = n, n-1, \dots, 1$:

$$\begin{aligned}
 c_k &= \bar{D}(-)a_k \quad (c_{kj} = \bar{D}_{jj}(-)a_{jk}, \quad j = 1, 2, \dots, 2n) \\
 D_{kk}(-) &= a^T c_k \\
 d_k &= c_k / D_{kk}(-) \\
 U_{jk}(-) &= a_j^T d_k \quad j = 1, 2, \dots, k-1 \\
 a_j &\leftarrow a_j - U_{jk}(-)a_k \quad j = 1, 2, \dots, k-1
 \end{aligned} \tag{54}$$

The final step of the U-D covariance factorization algorithm is the scalar measurement update. The following equations complete the update using the previously computed $U^T(-)$ and $D(-)$ matrices, the 1-by-n rows of the $H(t_i)$ matrix and the measurement covariance value.

$$\begin{aligned}
 f &= U^T H^T \\
 v_j &= D_{jj}(-)f_j \quad j = 1, 2, \dots, n \\
 a_o &= R
 \end{aligned} \tag{55}$$

Then, for $k = 1, 2, \dots, n$

$$\begin{aligned}
 a_k &= a_{k-1} + f_k v_k \\
 D_{kk}(+) &= D_{kk}(-)a_{k-1} / a_k \\
 b_k &\leftarrow v_k \\
 p_k &= -f_k / a_{k-1} \\
 U_{jk}(+) &= U_{jk}(-) + b_j p_k \quad j = 1, 2, \dots, k-1 \\
 b_j &\leftarrow b_j + U_{jk}(-)v_k \quad j = 1, 2, \dots, k-1
 \end{aligned} \tag{56}$$

The filter gain is then determined by

$$K = \frac{b}{a_n} \quad (57)$$

Finally, the state vector, $\hat{x}(+)$ and the covariance matrix, $P(+)$ can be determined using Eqns 27 and 28.

2.3 State Definition

The state for the cluster was initially composed of the position and velocity components with respect to the rotating reference point. That is, until Captain Ward discovered that the downrange, y , component of each satellite was unobservable. The component was removed from satellite #1's state and for satellites #2-s, the component was replaced with a relative down-range component measured with respect to satellite #1. The state vector for satellite #1 is updated to

$$\hat{x}_1 = \begin{bmatrix} x_1 \\ z_1 \\ \dot{x}_1 \\ \dot{y}_1 \\ \dot{z}_1 \end{bmatrix} \quad (58)$$

While the state vectors for satellites #2-s appear as

$$\hat{x}_i = \begin{bmatrix} x_i \\ \Delta y_i \\ z_i \\ \dot{x}_i \\ \dot{y}_i \\ \dot{z}_i \end{bmatrix} \quad i = 2, 3, \dots, s \quad (59)$$

Where Δy_i is determined by subtracting the y solution for satellites #2-s from the y solution for satellite #1.

Therefore,

$$\begin{aligned} \Delta y_i(+) &= y_1(+)-y_i(+)) \\ &= [6(\sin \psi - \psi)](x_1 - x_i) + (y_1(-) - y_i(-)) + (60) \\ &\quad \left[\frac{2}{\eta}(\cos \psi - 1) \right](\dot{x}_1 - \dot{x}_i) + \left(\frac{4}{\eta} \sin \psi - \frac{3\psi}{\eta} \right)(\dot{y}_1 - \dot{y}_i) \end{aligned}$$

The generalized state transition matrix, Φ , becomes

$$\Phi = \begin{bmatrix} \Phi_1 & 0 & 0 & \cdot & \cdot & 0 \\ \Phi_{12} & \Phi_2 & 0 & \cdot & \cdot & 0 \\ \Phi_{13} & 0 & \Phi_3 & \cdot & \cdot & 0 \\ \cdot & \cdot & \cdot & \cdot & \cdot & \cdot \\ \cdot & \cdot & \cdot & \cdot & \cdot & \cdot \\ \Phi_{1s} & 0 & 0 & \cdot & \cdot & \Phi_s \end{bmatrix} \quad (61)$$

Where

$$\Phi_1 = \begin{bmatrix} 4-3\cos \psi & 0 & \frac{\sin \psi}{\eta} & \frac{2}{\eta}(1-\cos \psi) & 0 \\ 0 & \cos \psi & 0 & 0 & \frac{\sin \psi}{\eta} \\ 3\eta \sin \psi & 0 & \cos \psi & 2\sin \psi & 0 \\ 6\eta(\cos \psi - 1) & 0 & -2\sin \psi & -3+4\cos \psi & 0 \\ 0 & -\eta \sin \psi & 0 & 0 & \cos \psi \end{bmatrix} \quad (62)$$

$$\Phi_i = \begin{bmatrix} 4-3\cos\psi & 0 & 0 & \frac{\sin\psi}{\eta} & \frac{2}{\eta}(1-\cos\psi) & 0 \\ -6(\sin\psi-\psi) & 1 & 0 & -\frac{2}{\eta}(\cos\psi-1) & -\frac{4}{\eta}\sin\psi + \frac{3\psi}{\eta} & 0 \\ 0 & 0 & \cos\psi & 0 & 0 & \frac{\sin\psi}{\eta} \\ 3\eta\sin\psi & 0 & 0 & \cos\psi & 2\sin\psi & 0 \\ 6\eta(\cos\psi-1) & 0 & 0 & -2\sin\psi & -3+4\cos\psi & 0 \\ 0 & 0 & -\eta\sin\psi & 0 & 0 & \cos\psi \end{bmatrix} \quad (63)$$

and

$$\Phi_{1i} = \begin{bmatrix} 0 & 0 & 0 & 0 & 0 & 0 \\ 6(\sin\psi-\psi) & 0 & \frac{2}{\eta}(\cos\psi-1) & \frac{4}{\eta}\sin\psi - \frac{3\psi}{\eta} & 0 & 0 \\ 0 & 0 & 0 & 0 & 0 & 0 \\ 0 & 0 & 0 & 0 & 0 & 0 \\ 0 & 0 & 0 & 0 & 0 & 0 \\ 0 & 0 & 0 & 0 & 0 & 0 \end{bmatrix} \quad (64)$$

Additionally, the h vector and the H matrix are modified to yield

$$h = \begin{bmatrix} \sqrt{(x_1-x_2)^2 + \Delta y_2^2 + (z_1-z_2)^2} \\ \vdots \\ \sqrt{(x_1-x_s)^2 + \Delta y_s^2 + (z_1-z_s)^2} \end{bmatrix} = \begin{bmatrix} h_1 \\ \vdots \\ h_{s-1} \end{bmatrix} \quad (65)$$

$$H = \begin{bmatrix} \bar{H}_1 & H_1 & 0 & \dots & 0 \\ \bar{H}_2 & 0 & H_2 & \dots & 0 \\ \vdots & \vdots & \vdots & \ddots & \vdots \\ \vdots & \vdots & \vdots & \vdots & \vdots \\ \bar{H}_{s-1} & 0 & 0 & \dots & H_{s-1} \end{bmatrix} \quad (66)$$

where

$$\tilde{H}_i = \begin{bmatrix} \frac{x_1 - x_{i+1}}{h_1} & \frac{z_1 - z_{i+1}}{h_1} & 0 & 0 & 0 \end{bmatrix} \quad (67)$$

$$H_i = \begin{bmatrix} -\left(\frac{x_1 - x_{i+1}}{h_i}\right) & \frac{\Delta y_{i+1}}{h_i} & -\left(\frac{z_1 - z_{i+1}}{h_i}\right) & 0 & 0 & 0 \end{bmatrix} \quad (68)$$

Once minor changes are made to the truth model and the estimator algorithms, the computer program is exactly as it was when Captain Ward generated his results.

III. Observability Analysis

The search for unobservable states was complicated by the use of the U-D covariance factorization algorithm, since the filter does not directly invert any matrices. Therefore, the filter was replaced by a non-linear least squares filter to take advantage of the fact that the matrix $\sum T^T Q^{-1} T$ (to be developed shortly) is inverted during the estimation process.

3.1 Non-Linear Least Squares Estimation

The equations of interest in the non-linear least squares problem are the update to the reference trajectory equation, the covariance of the estimate equation, and the residual equation. The update to the reference trajectory is given by:

$$\delta x(t_o) = (T^T Q^{-1} T)^{-1} T^T Q^{-1} r \quad (69)$$

Where for convenience the matrix product $H\Phi(t_i, t_o)$ was redefined as T . The vector r is the residual vector. The trajectory estimate is then given by:

$$\bar{x}(t_o) = x_{ref}(t_o) + \delta x(t_o) \quad (70)$$

The estimate covariance is given by:

$$P_{\delta x} = (T^T Q^{-1} T)^{-1} \quad (71)$$

Finally, the residual vector is given by the difference of the observed and the calculated data vector.

$$r = z - G(h(x(t_0), t_i), t_i) \quad (72)$$

The variables that appear on the right hand sides of the above equations were previously defined in Chapter 2. The inversion of the matrix product $T^T Q^{-1} T$ is the foundation of the calculations that appear in eqns 69-71. If the matrix is singular, a zero eigenvalue will exist (1:357), and the estimate covariance and the state update defined by eqns 69 and 71, respectively, will be undefined. In other words, unobservable states are present if the matrix is singular. Therefore, the ability to successfully invert the matrix $T^T Q^{-1} T$ is the key to the removal of the unobservable states.

3.2 Analysis

The analysis initially consisted of inverting the matrix $\sum T^T Q^{-1} T$ using a Gaussian elimination with maximal pivoting algorithm. Several assumptions were made to simplify the analysis: namely, the constellation consisted of only two satellites which greatly simplifies the problem; the data vector consisted not of the range between

the satellites, but consisted of the actual components of the state and the individual data measurements were considered independent and each equally contributing to the estimate to eliminate any questions about the data causing observability problems; and finally, the initial reference state was defined as the initial true state determined by the truth model thus reducing the analysis to a single iteration of the non-linear least squares estimation algorithm.

The first attempt to evaluate the inverse of $\sum T^T Q^{-1} T$ yielded a singular matrix as expected, confirming earlier suspicions of state unobservability. The next step was to redefine the state and update all equations defined with respect to the new state components (this task follows the steps outlined in Section 2.3). But which state components should be removed? An examination of the $\sum T^T Q^{-1} T$ matrix for which the Gaussian elimination process failed yielded a matrix of the following form.

$$\begin{bmatrix}
 X & X & X & X & X & X & X & X & X & X & X \\
 X & X & X & X & X & X & X & X & X & X & X \\
 X & X & X & X & X & X & X & X & X & X & X \\
 X & X & X & X & X & X & X & X & X & X & X \\
 X & X & X & X & X & X & X & X & X & X & X \\
 0 & 0 & 0 & 0 & 0 & 0 & 0 & 0 & 0 & 0 & 0 \\
 X & X & X & X & X & X & X & X & X & X & X \\
 0 & 0 & 0 & 0 & 0 & 0 & 0 & 0 & 0 & 0 & 0 \\
 0 & 0 & 0 & 0 & 0 & 0 & 0 & 0 & 0 & 0 & 0 \\
 0 & 0 & 0 & 0 & 0 & 0 & 0 & 0 & 0 & 0 & 0 \\
 0 & 0 & 0 & 0 & 0 & 0 & 0 & 0 & 0 & 0 & 0
 \end{bmatrix} \quad (73)$$

where X is a non-zero value. The z and \dot{z} components were removed in an assumption that an absolute horizontal plane of reference could not be determined.

The new state consists of the x , \dot{x} , and y components for satellites #1 and #2 and the relative components Δy , Δz , and $\Delta \dot{z}$ between satellites #1 and #2. The new equations for the non-linear least squares analysis assume the following form:

$$\hat{\mathbf{x}} = \begin{pmatrix} x_1 \\ \dot{x}_1 \\ y_1 \\ x_2 \\ \Delta y_2 \\ \Delta z_2 \\ \dot{x}_2 \\ y_2 \\ \Delta \dot{z} \end{pmatrix} = \mathbf{h} \quad (74)$$

$$\Phi = \begin{bmatrix} \Phi_1 & 0 \\ \Phi_{12} & \Phi_2 \end{bmatrix} \quad (75)$$

$$\Phi_1 = \begin{bmatrix} 4-3\cos\psi & \frac{\sin\psi}{\eta} & \frac{2}{\eta}(1-\cos\psi) \\ 3\eta\sin\psi & \cos\psi & 2\sin\psi \\ 6\eta(\cos\psi-1) & -2\sin\psi & -3+4\cos\psi \end{bmatrix} \quad (76)$$

$$\Phi_{12} = \begin{bmatrix} 0 & 0 & 0 \\ 6(\sin\psi-\psi) & \frac{2}{\eta}(\cos\psi-1) & \frac{4}{\eta}\sin\psi-\frac{3\psi}{\eta} \\ 0 & 0 & 0 \\ 0 & 0 & 0 \\ 0 & 0 & 0 \end{bmatrix} \quad (77)$$

$$\Phi_i = \begin{bmatrix} 4-3\cos\psi & 0 & 0 & \frac{\sin\psi}{\eta} & \frac{2}{\eta}(1-\cos\psi) & 0 \\ -6(\sin\psi-\psi) & 1 & 0 & -\frac{2}{\eta}(\cos\psi-1) & -\frac{4}{\eta}\sin\psi+\frac{3\psi}{\eta} & 0 \\ 0 & 0 & \cos\psi & 0 & 0 & \frac{\sin\psi}{\eta} \\ 3\eta\sin\psi & 0 & 0 & \cos\psi & 2\sin\psi & 0 \\ 6\eta(\cos\psi-1) & 0 & 0 & -2\sin\psi & -3+4\cos\psi & 0 \\ 0 & 0 & -\eta\sin\psi & 0 & 0 & \cos\psi \end{bmatrix} \quad (78)$$

Again, the inversion of $\sum T^T Q^{-1} T$ failed, yielding a singular matrix. The Gaussian elimination process reduced the matrix to

$$\begin{bmatrix}
 X & X & X & X & X & X & X & X & X \\
 X & X & X & X & X & X & X & X & X \\
 X & X & X & X & X & X & X & X & X \\
 0 & 0 & 0 & 0 & 0 & 0 & 0 & 0 & 0 \\
 X & X & X & X & X & X & X & X & X \\
 X & X & X & X & X & X & X & X & X \\
 0 & 0 & 0 & 0 & 0 & 0 & 0 & 0 & 0 \\
 0 & 0 & 0 & 0 & 0 & 0 & 0 & 0 & 0 \\
 X & X & X & X & X & X & X & X & X
 \end{bmatrix} \quad (79)$$

One may examine eqns 73 and 79 to conclude that the zero rows corresponding to the z_2 and \dot{z}_2 components were removed by introducing relative z and \dot{z} components into the state. Based upon this conclusion, the zero rows for the x_2, \dot{x}_2 , and \dot{y}_2 components may be removed by introducing relative $\Delta x, \Delta \dot{x}$, and $\Delta \dot{y}$ components into the state. This discovery warranted a re-examination of the solutions to the Clohessy-Wiltshire equations. If the solutions for satellite #1 and #2 are subtracted from each other and if like terms are collected, one obtains the following set of equations.

$$\Delta x(+) = (4 - 3\cos\psi)\Delta x_o(-) + \frac{\sin\psi}{\eta}\Delta \dot{x}_o(-) + \frac{2}{\eta}(1 - \cos\psi)\Delta \dot{y}_o(-) \quad (80)$$

$$\Delta y(+) = [6(\sin\psi - \psi)]\Delta x_o(-) + \Delta y_o(-) +$$

$$\frac{2}{\eta}(\cos\psi - 1)\Delta \dot{x}_o(-) + \left(\frac{4}{\eta}\sin\psi - \frac{3\psi}{\eta}\right)\Delta \dot{y}_o(-) \quad (81)$$

$$\Delta z(+) = \cos \psi \Delta z_o(-) + \sin \frac{\psi}{\eta} \Delta \dot{z}_o(-) \quad (82)$$

$$\Delta \dot{x}(+) = 3\eta \sin \psi \Delta x_o(-) + \cos \psi \Delta \dot{x}_o(-) + 2 \sin \psi \Delta \dot{y}_o(-) \quad (83)$$

$$\Delta \dot{y}(+) = 6\eta (\cos \psi - 1) \Delta x_o(-) - 2 \sin \psi \Delta \dot{x}_o(-) + (-3 + 4 \cos \psi) \Delta \dot{y}_o(-) \quad (84)$$

$$\Delta \dot{z}(+) = -\eta \sin \psi \Delta z_o(-) + \cos \psi \Delta \dot{z}_o(-) \quad (85)$$

This set of equations indicates that there is no possibility for determining the position and velocity state components separately for satellites #1 and #2 based upon a range measurement between the two satellites. For example, examining the $\Delta x(+)$ equation, an increase in the x_1, \dot{x}_1 , and \dot{y}_1 components and a corresponding increase in the x_2, \dot{x}_2 , and \dot{y}_2 components would yield the same solution as if no change had occurred at all. In other words, satellite #1, the filter's host satellite, considers itself at the origin of the reference frame and determines the relative motion of the other satellite with respect to itself. Once identified, the discovery seems obvious when one considers that range is a relative measurement and by itself does not yield any position information.

Equations 80-85 constitute the new dynamics model that the filter will use during the estimation process. The new state vector and state transition matrix for a cluster of s satellites assume the following form:

$$\hat{\mathbf{x}} = \begin{pmatrix} \Delta x_2 \\ \Delta y_2 \\ \Delta z_2 \\ \Delta \dot{x}_2 \\ \Delta \dot{y}_2 \\ \Delta \dot{z}_2 \\ \cdot \\ \cdot \\ \cdot \\ \Delta x_s \\ \Delta y_s \\ \Delta z_s \\ \Delta \dot{x}_s \\ \Delta \dot{y}_s \\ \Delta \dot{z}_s \end{pmatrix} = \begin{pmatrix} x_1 - x_2 \\ y_1 - y_2 \\ z_1 - z_2 \\ \dot{x}_1 - \dot{x}_2 \\ \dot{y}_1 - \dot{y}_2 \\ \dot{z}_1 - \dot{z}_2 \\ \cdot \\ \cdot \\ \cdot \\ x_1 - x_s \\ y_1 - y_s \\ z_1 - z_s \\ \dot{x}_1 - \dot{x}_s \\ \dot{y}_1 - \dot{y}_s \\ \dot{z}_1 - \dot{z}_s \end{pmatrix} \quad (86)$$

$$\hat{\mathbf{x}}(+) = \begin{bmatrix} \Phi & 0 & 0 & \cdot & \cdot & 0 \\ 0 & \Phi & 0 & \cdot & \cdot & 0 \\ 0 & 0 & \Phi & \cdot & \cdot & 0 \\ \cdot & \cdot & \cdot & \cdot & \cdot & \cdot \\ \cdot & \cdot & \cdot & \cdot & \cdot & \cdot \\ 0 & 0 & 0 & \cdot & \cdot & \Phi \end{bmatrix} \{\hat{\mathbf{x}}(-)\} \quad (87)$$

where

$$\Phi = \begin{bmatrix} 4 - 3\cos\psi & 0 & 0 & \frac{\sin\psi}{\eta} & \frac{2}{\eta}(1 - \cos\psi) & 0 \\ 6(\sin\psi - \psi) & 1 & 0 & \frac{2}{\eta}(\cos\psi - 1) & \frac{4}{\eta}\sin\psi - \frac{3\psi}{\eta} & 0 \\ 0 & 0 & \cos\psi & 0 & 0 & \frac{\sin\psi}{\eta} \\ 3\eta\sin\psi & 0 & 0 & \cos\psi & 2\sin\psi & 0 \\ 6\eta(\cos\psi - 1) & 0 & 0 & -2\sin\psi & -3 + 4\cos\psi & 0 \\ 0 & 0 & -\eta\sin\psi & 0 & 0 & \cos\psi \end{bmatrix} \quad (88)$$

Additionally, the h vector and the H matrix are now defined as

$$\mathbf{h} = \begin{bmatrix} \sqrt{\Delta x_2^2 + \Delta y_2^2 + \Delta z_2^2} \\ \cdot \\ \cdot \\ \cdot \\ \sqrt{\Delta x_s^2 + \Delta y_s^2 + \Delta z_s^2} \end{bmatrix} = \begin{bmatrix} h_2 \\ \cdot \\ \cdot \\ \cdot \\ h_s \end{bmatrix} \quad (89)$$

$$\mathbf{H} = \begin{bmatrix} \mathbf{H}_2 & 0 & 0 & \dots & 0 \\ 0 & \mathbf{H}_3 & 0 & \dots & 0 \\ \cdot & \cdot & \cdot & \cdot & \cdot \\ \cdot & \cdot & \cdot & \cdot & \cdot \\ \cdot & \cdot & \cdot & \cdot & \cdot \\ 0 & 0 & 0 & \dots & \mathbf{H}_s \end{bmatrix} \quad (90)$$

where

$$\mathbf{H}_i = \begin{bmatrix} \frac{\Delta x_i}{h_i} & \frac{\Delta y_i}{h_i} & \frac{\Delta z_i}{h_i} & 0 & 0 & 0 \end{bmatrix} \quad (91)$$

IV. Performance Analysis

Once the observable states are defined and the filter algorithm completed, the next step is to tune the filter and conduct a Monte Carlo simulation in order to assess the filter's performance. The tuning of the filter consists of varying the diagonal elements of the dynamics noise covariance matrix Q_d ; a rather simplified approach. Once the filter is adequately tuned, a Monte Carlo simulation will be conducted. The constellation size will be varied and so will the random number seed used to corrupt the range data. Fifteen test cases will be evaluated for constellations of two, five, and ten satellites. The positional errors between the truth model and the estimator will be determined at each time step. Average error versus time and average true error and filter covariance versus time plots will be generated. The average error should be near zero and the average true error and the filter covariance should be approximately equal.

The filter's performance is examined by comparing the values of the true error and the covariance of the estimate. The true error is the magnitude of the position difference between the truth model state and the estimate state.

$$\text{TRUE ERROR} = \sqrt{E_x^2 + E_y^2 + E_z^2} \quad (92)$$

where E_z is the difference between the Δx , Δy , or Δz component of the true state and the estimate state. The estimate's covariance is equal to the square root of the sum of the squares of the eigenvalues associated with the position components of the estimated state.

$$\sigma = \sqrt{(\text{Eigenvalue}(x))^2 + (\text{Eigenvalue}(y))^2 + (\text{Eigenvalue}(z))^2} \quad (93)$$

4.1 Filter Tuning

The first step in tuning the filter is to assess the filter's performance with the elements of the dynamics noise matrix set to zero. The true error and the covariance are plotted together in Figure 2 for approximately 20 orbits with a time step of 300 seconds. After the initial transient, the covariance exponentially decayed approaching zero. The estimate approaches perfection as the covariance approaches zero. Once the covariance reaches zero, the estimate will no longer change with time and a state of ignorance will exist concerning the future behavior of the estimated state. Therefore, the filter must be tuned so that the covariance on the average will neither decay to zero nor grow to infinity (7:84).

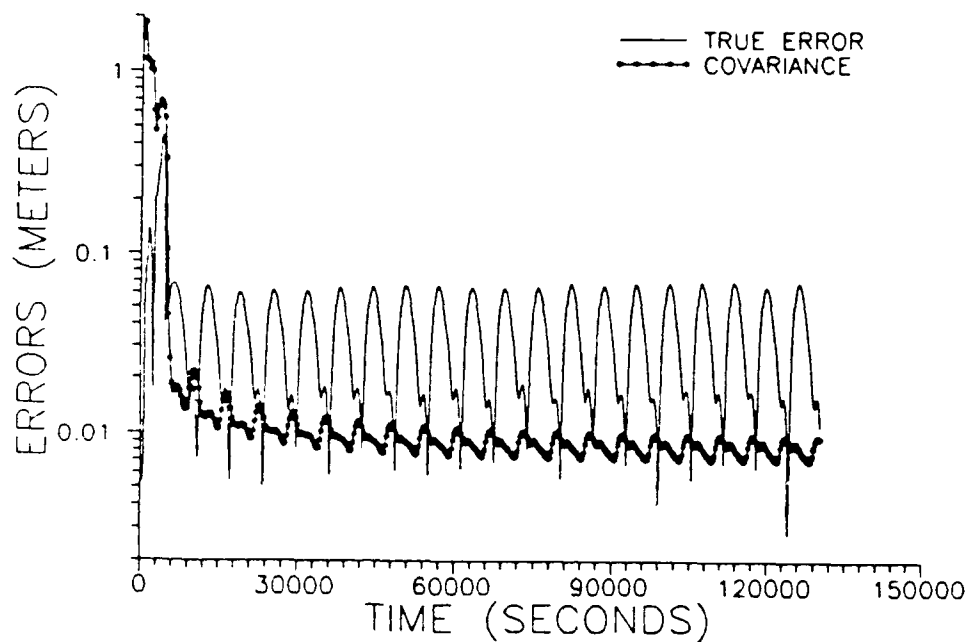


Figure 2. True error and covariance as a function of time with zero dynamics noise.

The process of tuning was confined to the diagonal elements of the dynamics noise covariance matrix Q_d with a constellation consisting of two satellites. The first task was to establish a ballpark initial value for the diagonal elements. The range between satellites was assumed to be accurate to within one centimeter. Therefore, one may

determine an acceleration value that will yield approximately a one centimeter error in position after one orbit by solving the following equation for a .

$$0.01 \text{ meters} = \frac{1}{2} a (\text{Period})^2 \quad (94)$$

The period is approximately 6300 seconds and the calculated value of " a " is approximately $5 \times 10^{-10} \text{ KM/SEC}^2$. Initially, only the diagonal elements corresponding to the relative velocity components were changed. Therefore, the elements assumed a value equal to:

$$Q_d = (a \Delta t_{\text{update}})^2 \quad (95)$$

The update time was 300 seconds and the new diagonal elements were approximately $2.25 \times 10^{-14} \text{ KM}^2/\text{SEC}^2$. The exponential decay of the zero dynamics noise filter was removed, but the true error curve was considerably below the covariance curve. Therefore, the filter was overestimating the error of the estimate (see Figure 3).

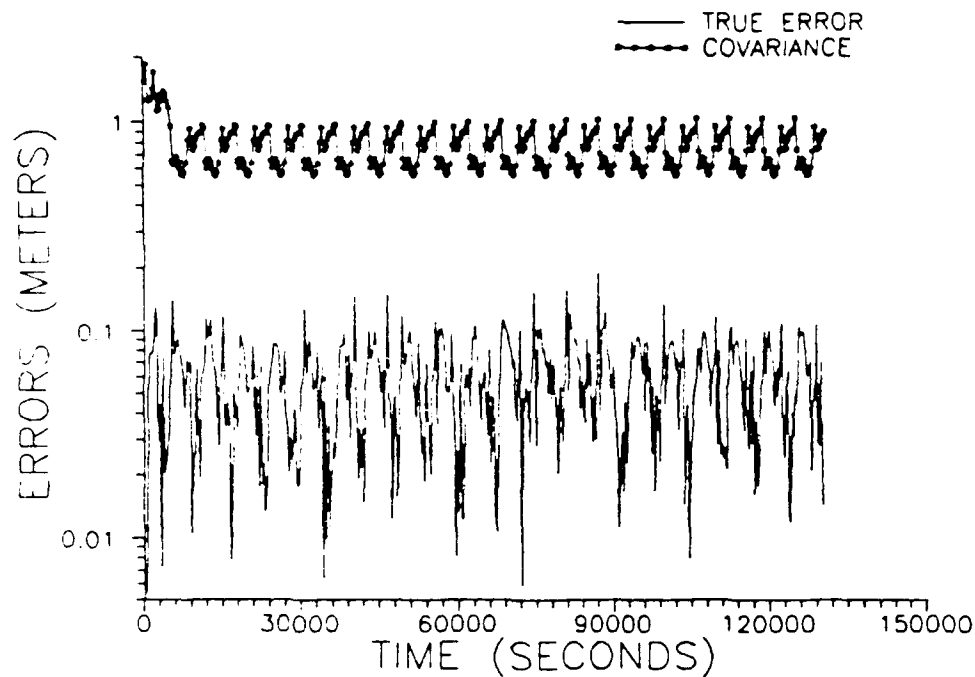


Figure 3. True error and covariance as a function of time with dynamics noise on the order of $2.25 \times 10^{-14} \text{ KM}^2/\text{SEC}^2$

Several values later, the filter was successfully tuned with an acceleration value of $1 \times 10^{-11} \text{ KM}/\text{SEC}^2$ and a noise covariance of $9 \times 10^{-18} \text{ KM}^2/\text{SEC}^2$. Figure 4 illustrates the desired result that the true error and the covariance curves overlap one another.

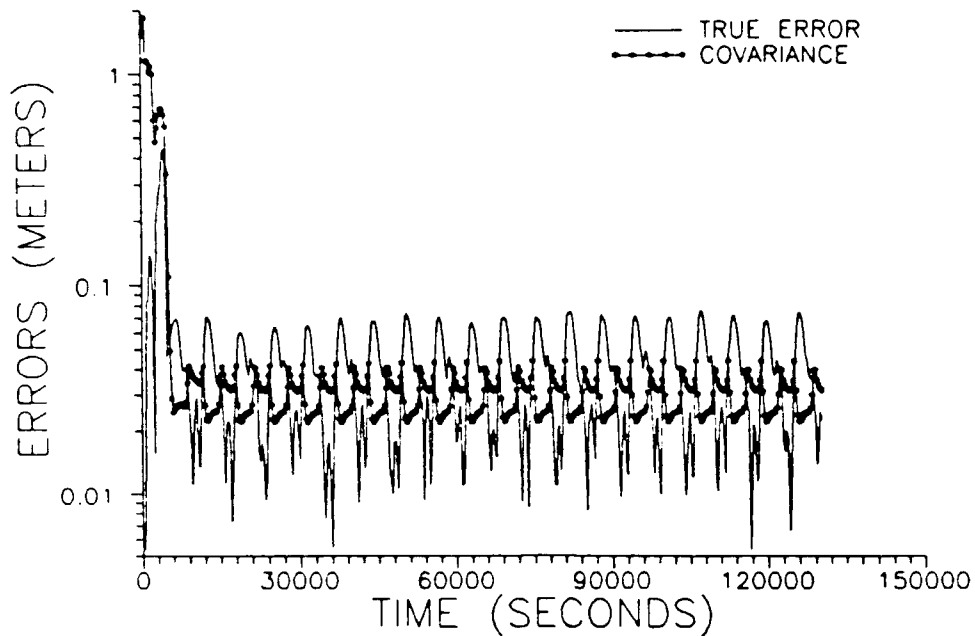


Figure 4. Filter tuned with dynamics noise covariance of $9 \times 10^{-18} \text{ KM}^2/\text{SEC}^2$.

The diagonal elements of the noise covariance matrix corresponding to the position components were varied but did not yield any appreciable benefits. For all subsequent testing, these elements remained set to zero.

4.2 Monte Carlo Simulation

Once the filter was successfully tuned, a 15-sample Monte Carlo simulation was conducted for constellations of

2, 5, and 10 satellites. The purpose of the simulation is to test the filter's performance based upon varying initial conditions. The truth model generated the true state and the range data between the host satellite and the remaining satellites at each time step. The initial estimator state was set equal to the initial state determined from the truth model. The random number generator seed used during the corruption of the range data was changed for each simulation run. For each constellation size and for each simulation run, the positional errors between the truth model and the estimator, and the filter covariance were calculated and stored within separate data files. The final results consisted of an average error, an average true error, and the filter covariance at each time step. For constellations of 5 and 10 satellites, the average errors and covariance were determined for three different groupings of satellites. For example, the error data was calculated between satellites #1 and #2, #1 and #3, and #1 and #5 for the five satellite constellation.

The average error is determined by summing the positional errors from the 15 data files for each time step and dividing by 15.

$$\bar{E} = \frac{1}{15} \sum_{i=1}^{15} (E_x + E_y + E_z)_i \quad (96)$$

The average true error is determined by summing the square of the positional errors from the data files, dividing by 15 and taking the square root.

$$\bar{E}_T = \sqrt{\frac{1}{15} \sum_{i=1}^{15} (E_x^2 + E_y^2 + E_z^2)_i} \quad (97)$$

The covariance calculated by the estimator at each time step is recorded in an additional data file. The average error should be approximately equal to zero and the average true error and the filter covariance should be approximately equal.

4.2.1 Two Satellite Cluster

Figures 5 and 6 depict the average error and the average true error and covariance results for a two satellite cluster. As expected the average error curve is near zero and the average true error and the filter covariance curves are nearly equal as a function of time. The average true error approaches a value of approximately 3 centimeters or three times the range measurement error and is well within the 25 meter accuracy requirement (3:vii). The steady state filter performance exhibits an oscillatory nature with a period equal to the orbital period of the cluster (approximately 6300 seconds).

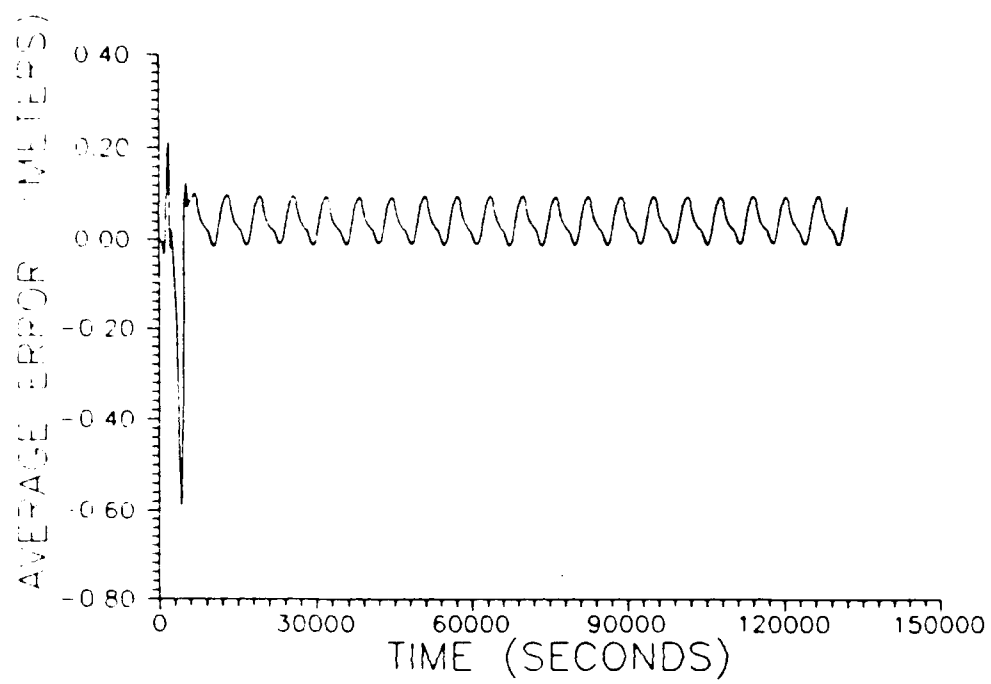


Figure 5. Average error versus time for a two satellite cluster.

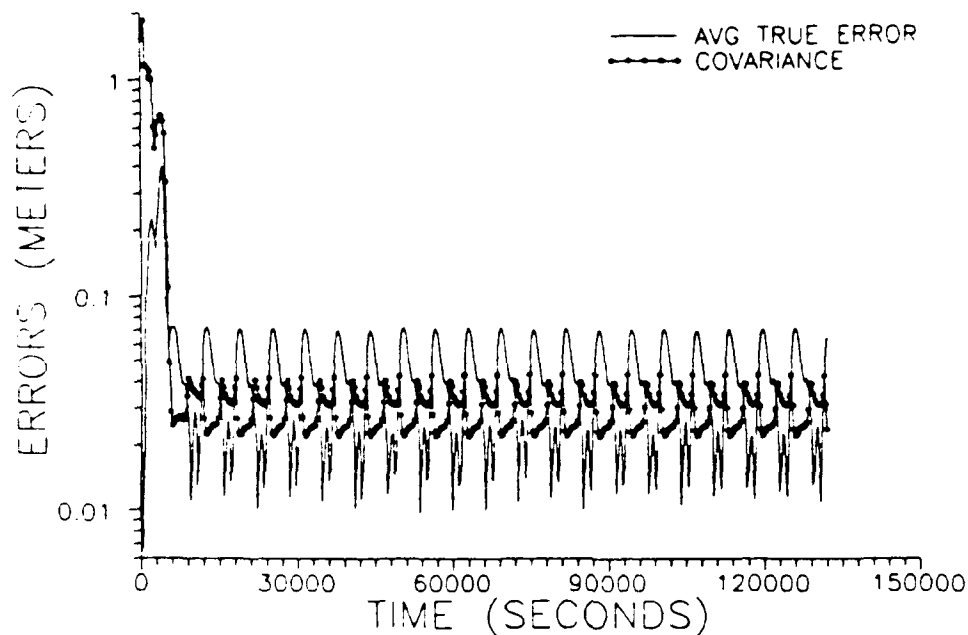


Figure 6. Comparison of average true error and covariance versus time for a two satellite cluster.

4.2.2 Five Satellite Cluster

Figures 7-12 depict the average error and the average true error and covariance results for a five satellite cluster. The filter was not re-tuned. The diagonal values of the dynamics noise matrix from the 'tuned' two satellite constellation case were assigned to the diagonal elements of the three additional satellites. Figures 7 and 8 are the error plots for relative position determination between satellites one and two. Figures 9

and 10 are the error plots for relative position determination between satellites one and three. Figures 11 and 12 are the error plots for relative position determination between satellites one and five. The filter performs as desired with an average true error on the order of two to three times the range measurement error. The filter continues to exhibit the oscillatory behavior previously noted.

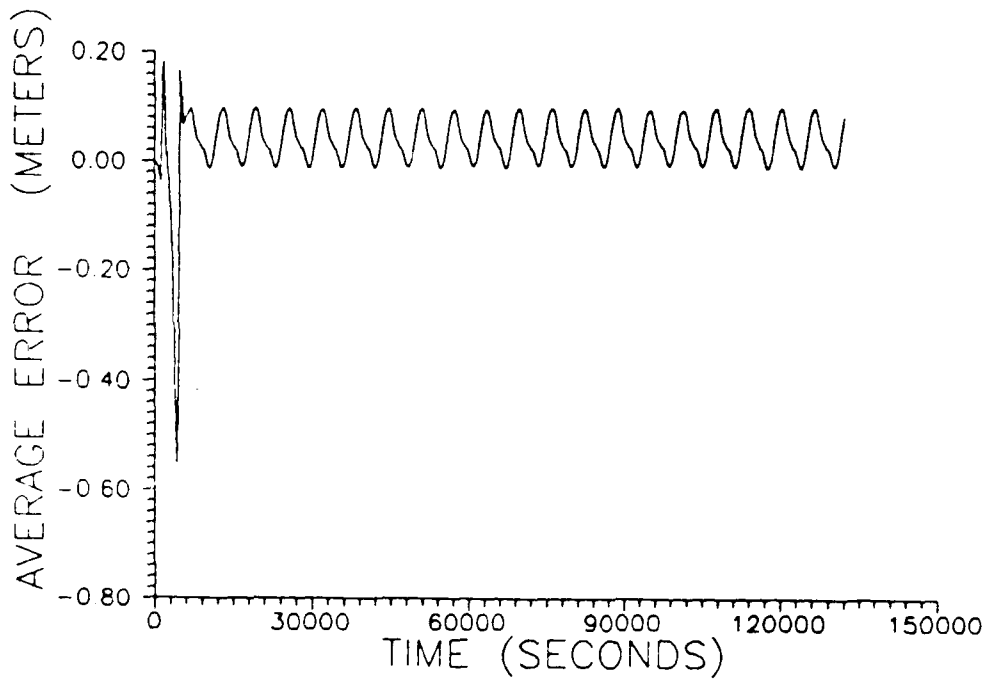


Figure 7. Average error between satellites 1 and 2.

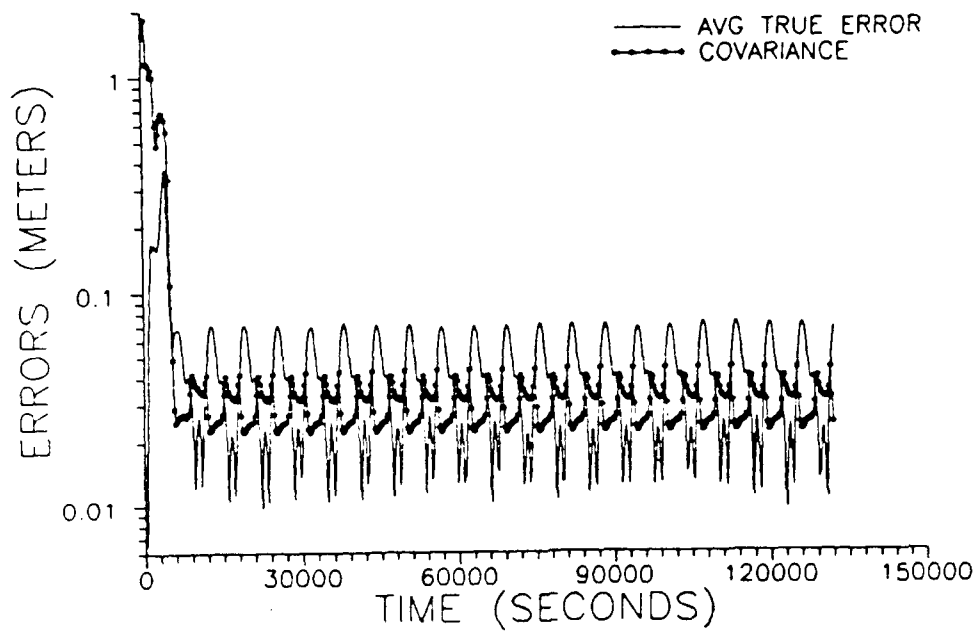


Figure 8. Comparison of average true error and covariance versus time for satellites 1 and 2.

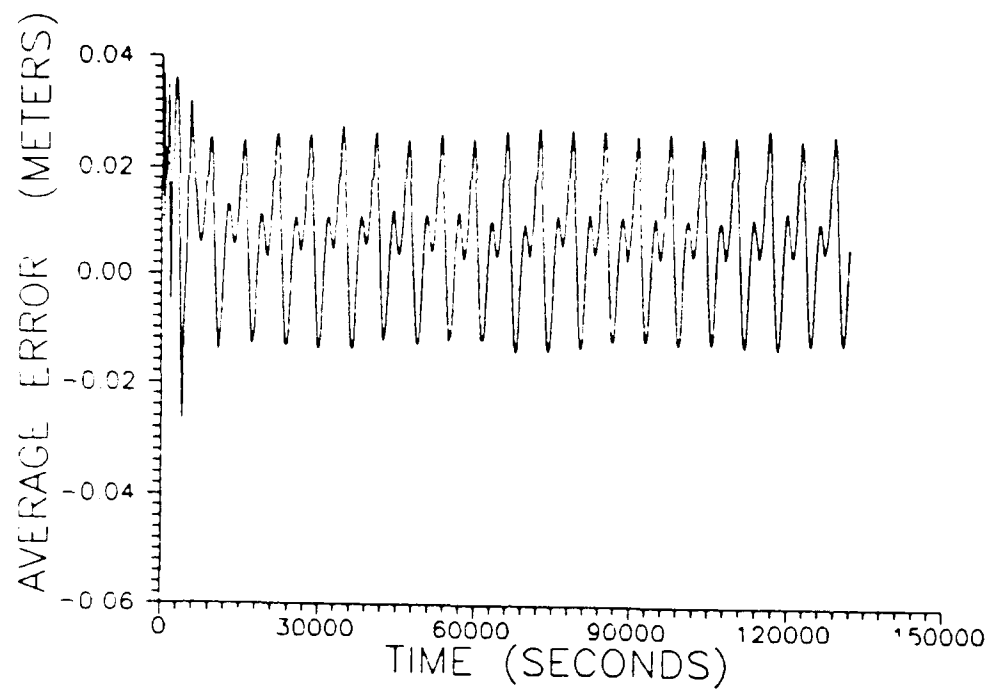


Figure 9. Average error between satellites 1 and 3.

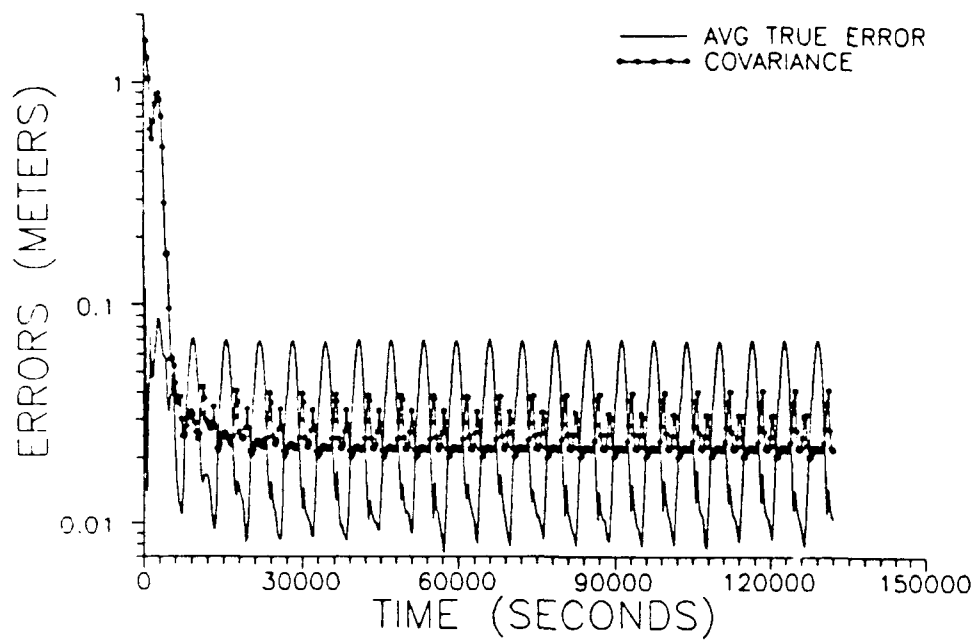


Figure 10. Comparison of average true error and covariance versus time for satellites 1 and 3.

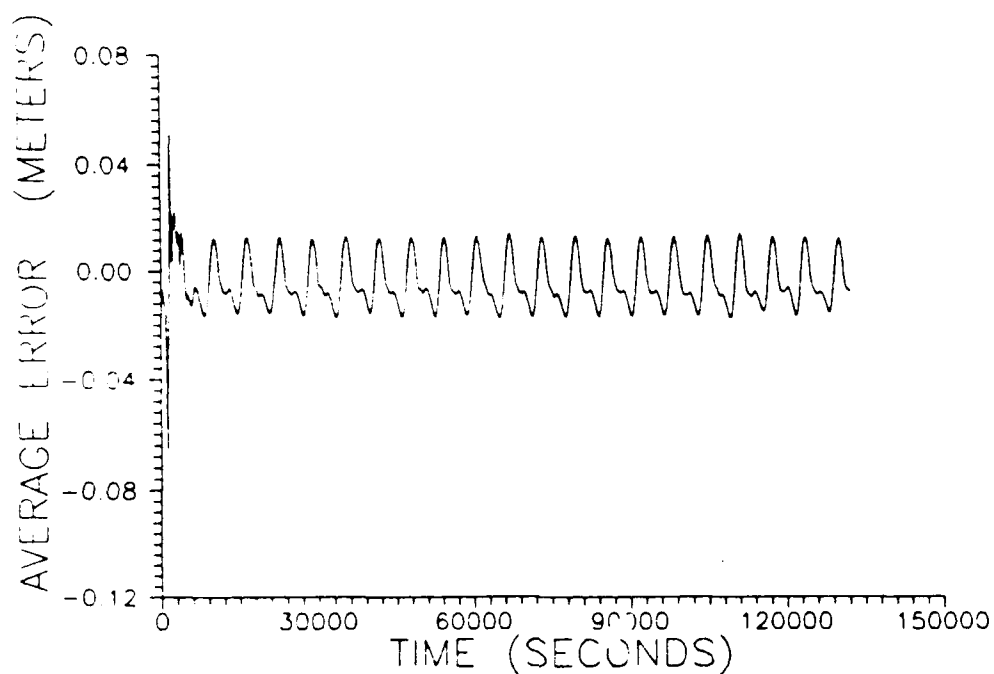


Figure 1. Average error between satellites 1 and 5.

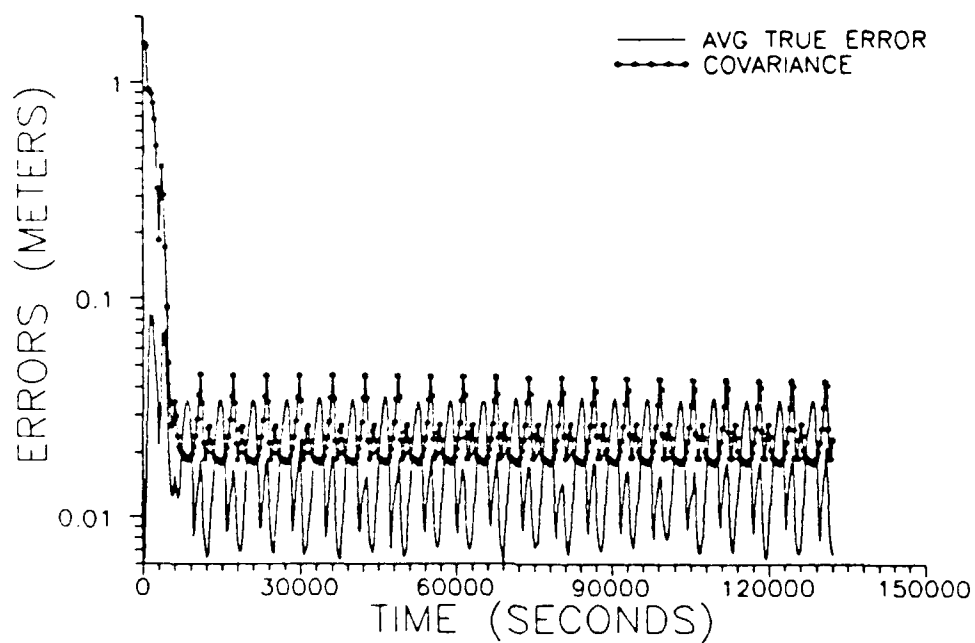


Figure 12. Comparison of average true error and covariance versus time for satellites 1 and 5.

4.2.3 Ten Satellite Cluster

Figures 13-18 depict the average error and the average true error and covariance results for a ten satellite cluster. Again, the filter was not re-tuned and the additional diagonal elements of the dynamics noise matrix were assigned the same values as previously used. Figures 13 and 14 are the error plots for relative position determination between satellites one and two. Figures 15 and 16 are the error plots for relative position determination between satellites one and five. Figures 17 and 18 are the error plots for relative position determination between satellites one and ten. The expected data trends are obtained for the ten satellite cluster case. The average true errors are approximately two to three times the range measurement error and again the oscillatory behavior of the filter is exhibited as previously discussed.

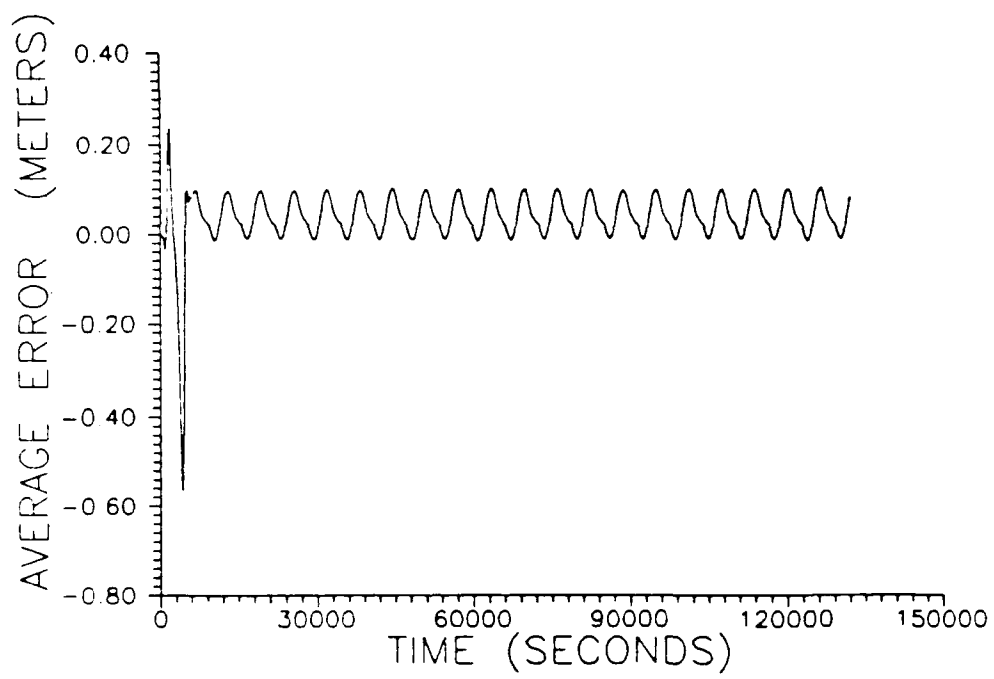


Figure 13. Average error between satellites 1 and 2.

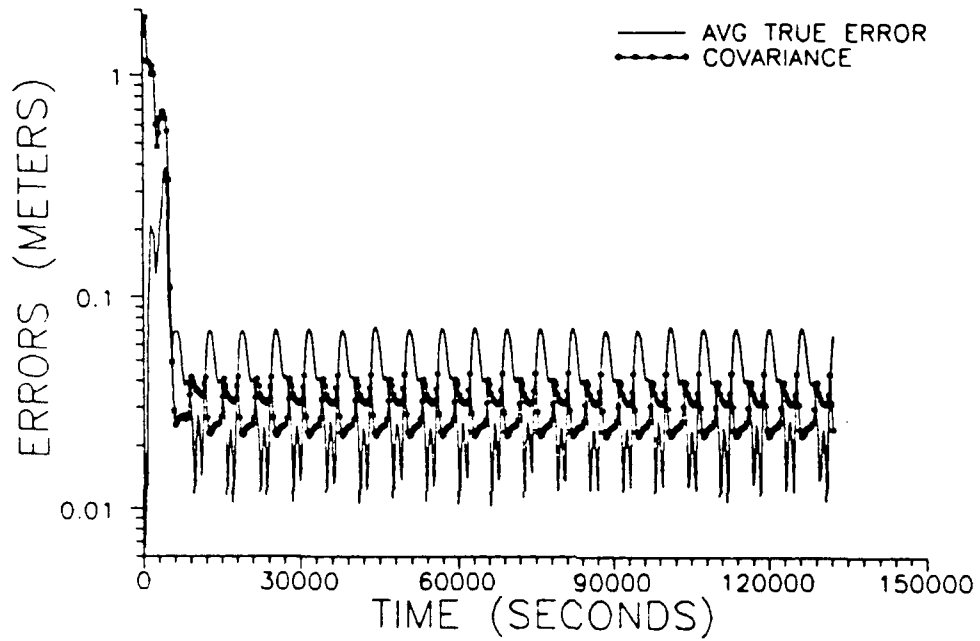


Figure 14. Comparison of average true error and covariance versus time for satellites 1 and 2.

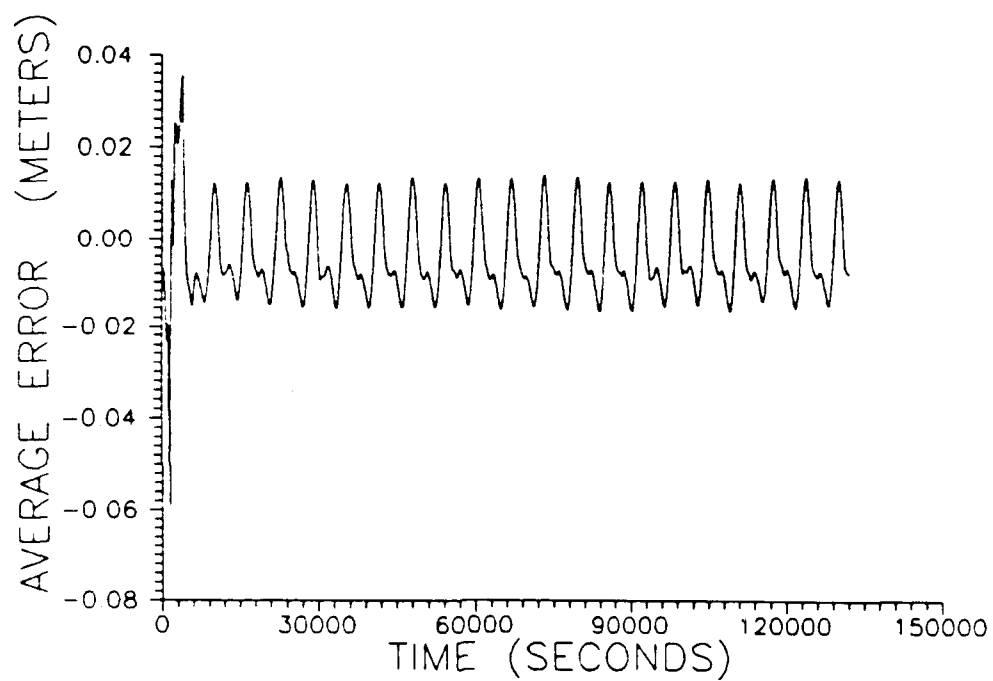


Figure 15. Average error between satellites 1 and 5.

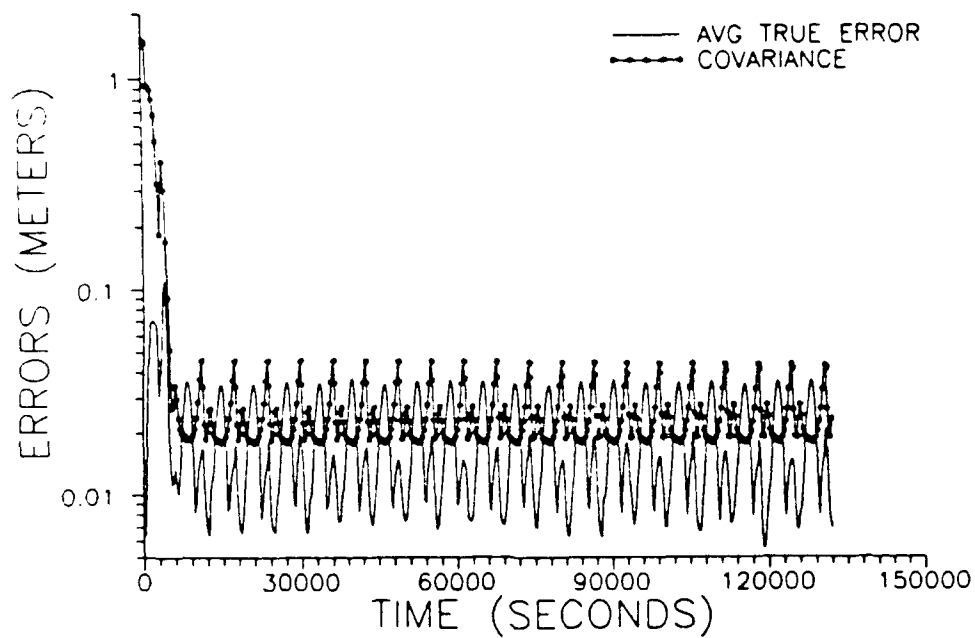


Figure 16. Comparison of average true error and covariance versus time for satellites 1 and 5.

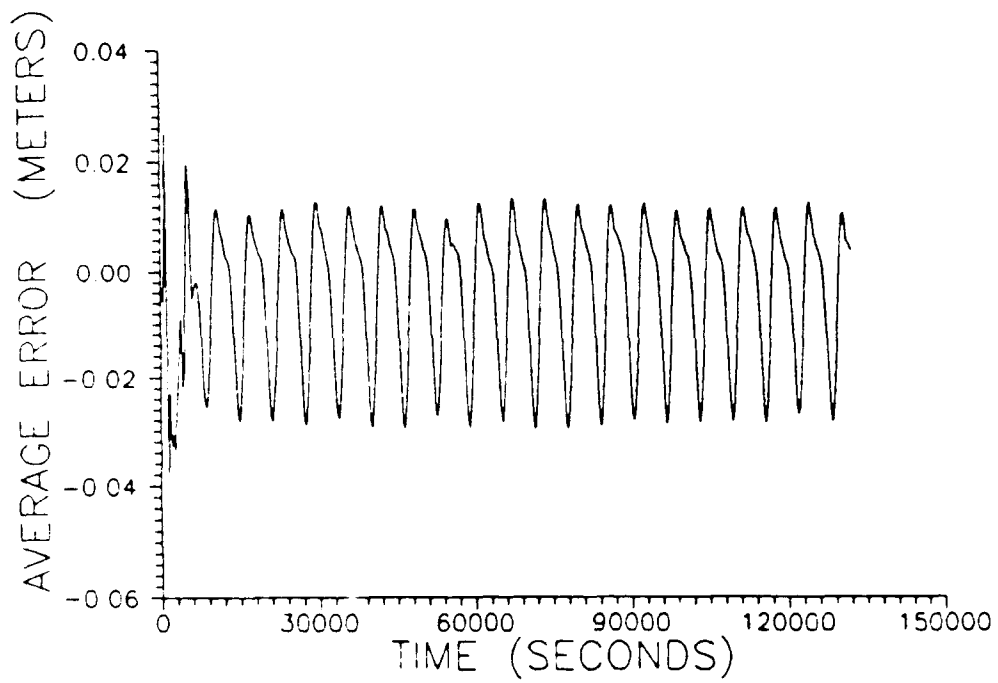


Figure 17. Average error between satellites 1 and 10.

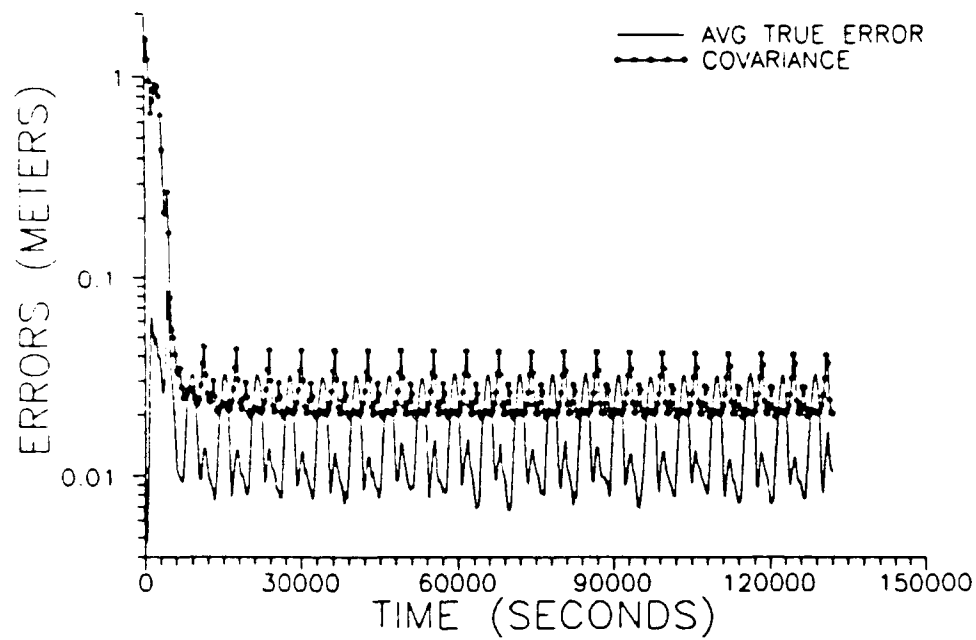


Figure 18. Comparison of average true error and covariance versus time for satellites 1 and 10.

V. Conclusions and Recommendations

Relative position determination of a satellite cluster using an on-board estimator is possible and yields good results tested against a two-body astrodynamics model. The state of the cluster can only involve relative position and velocity components between the filter host satellite and the remaining satellites. The U-D Covariance Factorization Kalman Filter was tuned and subjected to a 15-sample Monte Carlo Simulation. The error results presented illustrate good behavior of the average error, the average true error, and the filter covariance. The average true errors were approximately three times the range measurement error.

Further investigations into this topic should include a full tuning analysis, a filter robustness test, a test of the filter's performance using a more accurate truth model and an investigation into the filter's cyclic behavior. The variation of non-diagonal components of the dynamics noise covariance matrix should be investigated for any significant gain in performance or accuracy. A full test of the filter's robustness should be conducted to analyze the filter's performance with a poor initial guess for the initial state, and with periods of highly inaccurate range data. A test with an extremely accurate

perturbations model for the truth model should be conducted as a preliminary test to establish the filter's flight-readiness. Finally, the filter's cyclic behavior should be investigated to fully understand the filter's performance.

Bibliography

1. Agnew, Jeanne and Robert C. Knapp. Linear Algebra With Applications. Monterey, CA: Brooks/Cole Publishing Co, 1978.
2. Bate, Roger and others. Fundamentals of Astrodynamics. New York: Dover Publications, 1971.
3. Filer, Captain Sherrie Norton. Investigation of the Observability of a Satellite Cluster in a Near Circular Orbit. MS thesis, AFIT/GA/eny/89D-2, School of Engineering, Air Force Institute of Technology (AU), Wright-Patterson AFB OH, December 1989.
4. Maybeck, Peter S. Stochastic Models, Estimation, and Control Volume 1. New York: Academic Press, 1979.
5. Maybeck, Peter S. Stochastic Models, Estimation, and Control Volume 2. New York: Academic Press, 1982.
6. Ward, Captain Michael L. P. Estimated Satellite Cluster Elements in Near Circular Orbit. MS thesis, AFIT/GA/AA/88D-13, School of Engineering, Air Force Institute of Technology (AU), Wright-Patterson AFB OH, December 1988.
7. Wiesel, William B. Class handout distributed in MECH 731, Modern Methods of Orbit Determination. School of Engineering, Air Force Institute of Technology (AU), Wright-Patterson AFB OH, April 1990.

Bibliography

8. Wiesel, William B. Spaceflight Dynamics. New York:
McGraw-Hill, 1989.

VITA

Captain Stephen C. Johnston was born 6 February 1960 in Enid, Oklahoma. He graduated from Mesa High School in Mesa, Arizona in 1978. Later he attended Arizona State University, from which he received a degree of Bachelor of Science in Physics. Upon graduation, he attended Officer Training School at Lackland AFB TX and was commissioned a Second Lieutenant on 15 February 1983. He was assigned to the Engineering Conversion Program and attended Auburn University in Auburn, Alabama. He graduated with a degree of Bachelor of Science in Aerospace Engineering. Upon graduation, he was assigned to the Air Force Satellite Control Facility, Sunnyvale AFS CA. He was assigned to several satellite programs including the Anti-Satellite/Instrumented Test Vehicle program. He departed as the Division's Chief of Operations in April 1989 to attend the School of Engineering at the Air Force Institute of Technology.

Permanent address:

3847 Hillsboro Drive
Beavercreek, Ohio 45431

REPORT DOCUMENTATION PAGE

FORM Approved

DA Form 290-1088

This report is prepared in accordance with the instructions for the preparation of reports, including the time for reviewing instructions, gathering existing data sources, gathering and maintaining the data needed, completing the review, and preparing the report. Send comments regarding this burden estimate or any other aspect of this collection of information, including suggestions for reducing the burden, to Washington Headquarters Service, Directorate for Information Operations and Reports, 1215 Jefferson Davis Highway, Suite 1204, Arlington, VA 22202-4302, and to the Office of Management and Budget, Paperwork Reduction Project (0704-0188), Washington, DC 20503.

1. AGENCY USE ONLY (Leave blank)		2. REPORT DATE December 1990	3. REPORT TYPE AND DATES COVERED Master's Thesis
4. TITLE AND SUBTITLE AUTONOMOUS NAVIGATION OF A SATELLITE CLUSTER			5. FUNDING NUMBERS
6. AUTHOR(S) Stephen C. Johnston, Capt, USAF			
7. PERFORMING ORGANIZATION NAME(S) AND ADDRESS(ES) Air Force Institute of Technology WPAFB, OH 45433-6580			8. PERFORMING ORGANIZATION REPORT NUMBER AFIT/GA/ENY/90D-9
9. SPONSORING/MONITORING AGENCY NAME(S) AND ADDRESS(ES)			10. SPONSORING/MONITORING AGENCY REPORT NUMBER
11. SUPPLEMENTARY NOTES			
12a. DISTRIBUTION/AVAILABILITY STATEMENT Approved for public release; distribution unlimited			12b. DISTRIBUTION CODE
13. ABSTRACT (Maximum 200 words) The relative position determination of a cluster of satellites operating in a low earth orbit is investigated. A U-D Covariance Factorization Kalman Filter is used for the on-board estimator with dynamics based on the Clohessy-Wiltshire equations. Measurements consist of range data between a single host satellite and the remaining cluster. Therefore only relative position and velocity states with respect to the host satellite can be determined. A 15 sample Monte Carlo simulation was conducted with clusters of 2, 5, and 10 satellites, respectively. Performance results consists of average error, average true error and filter covariance as a function of time. <i>Keywords:</i>			
14. SUBJECT TERMS Satellite Cluster, Kalman Filter, <i>Navigation, (TRD)</i>			15. NUMBER OF PAGES 65
			16. PRICE CODE
17. SECURITY CLASSIFICATION OF REPORT Unclassified	18. SECURITY CLASSIFICATION OF THIS PAGE Unclassified	19. SECURITY CLASSIFICATION OF ABSTRACT Unclassified	20. LIMITATION OF ABSTRACT UL

GENERAL INSTRUCTIONS FOR COMPLETING SF 298

The Report Documentation Page (RDP) is used in announcing and cataloging reports. It is important that this information be consistent with the rest of the report, particularly the cover and title page. Instructions for filling in each block of the form follow. It is important to **stay within the lines to meet optical scanning requirements.**

Block 1. Agency Use Only (Leave Blank)

Block 2. Report Date. Full publication date including day, month, and year, if available (e.g. 1 Jan 88). Must cite at least the year.

Block 3. Type of Report and Dates Covered. State whether report is interim, final, etc. If applicable, enter inclusive report dates (e.g. 10 Jun 87 - 30 Jun 88).

Block 4. Title and Subtitle. A title is taken from the part of the report that provides the most meaningful and complete information. When a report is prepared in more than one volume, repeat the primary title, add volume number, and include subtitle for the specific volume. On classified documents enter the title classification in parentheses.

Block 5. Funding Numbers. To include contract and grant numbers; may include program element number(s), project number(s), task number(s), and work unit number(s). Use the following labels:

C - Contract	PR - Project
G - Grant	TA - Task
PE - Program Element	WU - Work Unit Accession No.

Block 6. Author(s). Name(s) of person(s) responsible for writing the report, performing the research, or credited with the content of the report. If editor or compiler, this should follow the name(s).

Block 7. Performing Organization Name(s) and Address(es). Self-explanatory.

Block 8. Performing Organization Report Number. Enter the unique alphanumeric report number(s) assigned by the organization performing the report.

Block 9. Sponsoring/Monitoring Agency Names(s) and Address(es). Self-explanatory.

Block 10. Sponsoring/Monitoring Agency Report Number. (If known)

Block 11. Supplementary Notes. Enter information not included elsewhere such as: Prepared in cooperation with...; Trans. of ..., To be published in When a report is revised, include a statement whether the new report supersedes or supplements the older report.

Block 12a. Distribution/Availability Statement. Denote public availability or limitation. Cite any availability to the public. Enter additional limitations or special markings in all capitals (e.g. NOFORN, REL, ITAR)

DOD - See DoDD 5230.24, "Distribution Statements on Technical Documents."

DOE - See authorities

NASA - See Handbook NHB 2200.2.

NTIS - Leave blank.

Block 12b. Distribution Code.

DOD - DOD - Leave blank

DOE - DOE - Enter DOE distribution categories from the Standard Distribution for Unclassified Scientific and Technical Reports

NASA - NASA - Leave blank

NTIS - NTIS - Leave blank.

Block 13. Abstract. Include a brief (Maximum 200 words) factual summary of the most significant information contained in the report.

Block 14. Subject Terms. Keywords or phrases identifying major subjects in the report.

Block 15. Number of Pages. Enter the total number of pages.

Block 16. Price Code. Enter appropriate price code (NTIS only).

Blocks 17. - 19. Security Classifications. Self-explanatory. Enter U.S. Security Classification in accordance with U.S. Security Regulations (i.e., UNCLASSIFIED). If form contains classified information, stamp classification on the top and bottom of the page.

Block 20. Limitation of Abstract. This block must be completed to assign a limitation to the abstract. Enter either UL (unlimited) or SAR (same as report). An entry in this block is necessary if the abstract is to be limited. If blank, the abstract is assumed to be unlimited.